Published in final edited form as:
Cancer Res. 2011 August 1; 71(15): 5154–5163. doi:10.1158/0008-5472.CAN-10-4513.

IGFBP-3 is a Metastasis Suppression Gene in Prostate Cancer

Hemal H. Mehta[1], **Qinglei Gao**[1], **Colette Galet**[2], **Vladislava Paharkova**[1], **Junxiang Wan**[1], **Jonathan Said**[3], **Joanne J. Sohn**[4], **Gregory Lawson**[4], **Pinchas Cohen**[1], **Laura J. Cobb**[1], and **Kuk-Wha Lee**[1]

[1]Pediatric Endocrinology, Mattel Children's Hospital, David Geffen School of Medicine at UCLA, Los Angeles, CA 90095 USA

[2]Department of Urology, David Geffen School of Medicine at UCLA, Los Angeles, CA 90095 USA

[3]Deparment of Pathology and Laboratory Medicine, David Geffen School of Medicine, Los Angeles, CA 90095 USA

[4]Division of Laboratory Animal Medicine, David Geffen School of Medicine, Los Angeles, CA 90095 USA

Abstract

The insulin-like growth factor binding protein IGFBP-3 is a pro-apoptotic and anti-angiogenic protein in prostate cancer (CaP). Epidemiological studies suggest that low IGFBP-3 is associated with greater risk of aggressive, metastatic prostate cancers, but *in vivo* functional data are lacking. Here we show that mice that are genetically deficient in IGFBP-3 exhibit weaker growth of primary prostate tumors growth but higher incidence of metastatic disease. Prostates in IGFBP-3 knockout mice (IGFBP-3KO mice) failed to undergo apoptosis after castration. Spontaneous prostate tumors did not develop in IGFBP-3KO mice, but splenic lymphomas occured in 23% of female IGFBP-3KO mice by 80 weeks of age. To assess the effects of IGFBP-3 deficiency on prostate cancer development, we crossed IGFBP-3KO mice with a c-Myc-driven model of CaP that develops slow-growing, non-metastatic tumors. By 24 weeks of age, well-differentiated prostate cancers were observed in all mice regardless of IGFBP-3 status. However, by 80 weeks of age IGFBP-3KO mice tended to exhibit larger prostate tumors than control mice. More strikingly, lung metastases were observed at this time in 55% of the IGFBP-3KO mice but none of the control animals. Cell lines established from Myc:IGFBP-3KO tumors displayed more aggressive phenotypes in proliferation, invasion and colony formation assays, relative to control Myc tumor cell lines. In addition, Myc:IGFBP-3KO cells exhibited evidence of epithelial-mesenchymal transition (EMT). Our findings establish a function for IGFBP-3 in suppressing metastasis in prostate cancer, and they also offer the first reported transgenic model of spontaneous metastatic prostate cancer for studies of this advanced stage of disease.

Keywords

IGFBP-3; metastasis; knockout mouse; prostate cancer

Address for Correspondence: Kuk-Wha Lee Department of Pediatrics Division of Endocrinology Mattel Children's Hospital 10833 Le Conte Ave, 22-315 MDCC Los Angeles, CA 90095-1752 Phone: (310) 825-6980 Fax: (310) 206-5843 kukwhalee@mednet.ucla.edu.

Disclosure Statement: The authors have nothing to disclose.

Introduction

The acquired capability of tumor cells for tissue invasion and metastasis has been defined as a “hallmark of cancer” (1) and currently no curative therapies exist for prostate cancer (CaP) that has metastasized (2). A chemotherapeutic agent, docetaxel, is the only approved therapy that has been shown to prolong survival among men with this condition (3); although a recent study reports improved survival among men with metastatic castration-resistant prostate cancer with use of Sipuleucel-T, an autologous active cellular immunotherapy (4). Despite these advances, the molecular mechanisms that underlie the process of metastasis are poorly understood.

Tumor-suppressive properties of Insulin-like Growth Factor Binding Protein (IGFBP)-3 (for review see (5)) include sequestration of the IGFs (6) and senescence association (7). In addition, IGFBP-3 has a clear inhibitory effect on tumor cell adhesion to extracellular matrix components in the presence and absence of IGF (8). Indeed, it was identified by microarray analysis as the most reduced transcript in CaP cells obtained through laser micro-dissection relative to neighboring normal prostatic cells (9). We published evidence that demonstrated the anti-angiogenic and pro-apoptotic effects of IGFBP-3 on CaP *in vivo* (10, 11).

Several clinical studies have shown that serum IGF-I is elevated and IGFBP-3 levels reduced in patients before the diagnosis of CaP and that increased serum levels of IGFBP-3 are associated with a decreased risk and better prognosis of CaP (12-14). Importantly, an IGFBP-3 promoter polymorphism has been associated with increasing risk for CaP metastasis and for having tumors with a biologically more aggressive phenotype (15).

We studied the effect of crossing mice with a genetic deletion of IGFBP-3 with mice expressing human *Myc* in the prostate (16). These *Myc* mice reliably develop murine prostatic intraepithelial neoplasia, then locally invasive adenocarcinomas. Additionally, these tumors share molecular features with human prostate cancer. We describe an important requirement for IGFBP-3 in prostate apoptosis induced by androgen deprivation, and identify a role for IGFBP-3 as a metastasis suppression gene.

Materials and Methods

Mouse Colony, Castration, Tissue Collection, Preparation, and Necropsy

Animal experiments were approved by the Animal Research Committee (ARC) of the University of California, Los Angeles and according to NIH guidelines. IGFBP-3KO and WT mice were bred and homozygous littermates were used in the study. Male and female pups were weaned, weighed, and genotyped at 3 weeks of age and maintained on normal chow.

Ten-week-old adult male mice were castrated or sham- operated in survival surgeries and the ventral and dorsolateral prostate was removed after 2 or 3 days. Briefly, animals were anesthetized with metophane, a lateral incision was made into the scrotum and the testes ligated and removed. The incision was closed with surgical silk.

Prostates and testes were fixed and stained with H&E for morphologic analysis and quantification of apoptosis using a TUNEL strategy (see below). TUNEL staining was performed according to established procedures (10). Apoptosis was quantitated by scoring 500 epithelial cells per field in five random fields per tissue section.

Tissues collected at necropsy were routinely fixed in 10% (v/v) phosphate-buffered formalin for 6 h and then transferred to 70% ethanol. Sections were cut from paraffin-embedded tissues and mounted on slides. Routine sections were stained with H&E.

Generation of IGFBP-3KO:Myc and WT:Myc Mice

The PB-Hi-Myc (Myc) mouse was derived at UCLA and was a kind gift of Dr. Charles Sawyers (16). These were bred with IGFBP3KO mice, originally developed in collaboration with Lexicon Pharmaceuticals, Inc. (17). The Myc model was generated by utilizing the probasin promoter (ARR2PB) to target the myc gene to the mouse prostate. To avoid potential genetic variations, only F3 generation of male offspring was used in this study.

Genotyping

Female Myc mice were crossed with male IGFBP-3 KO mice to produce the F1 generation. F1 mice, heterozygous for *myc* transgene and *igfpbp-3* gene (IGFBP-$3^{+/-}$Myc$^{+/-}$) were mated with heterozygous IGFBP-3 (BP-$3^{+/-}$ Myc$^{-/-}$) mice to generate F2 mice. The expected F2 genotypes were IGFBP-$3^{+/+}$Myc$^{+/-}$, IGFBP-$3^{+/+}$Myc$^{-/-}$, IGFBP-$3^{-/-}$Myc$^{+/-}$, IGFBP-$3^{-/-}$Myc$^{-/-}$, IGFBP-$3^{+/-}$ Myc$^{+/-}$, and IGFBP-$3^{+/-}$ Myc$^{-/-}$. IGFBP-3KO:Myc (IGFBP-$3^{-/-}$Myc$^{+/-}$) of F2 and subsequent generations will be mated with their IGFBP-3KO (IGFBP-$3^{-/-}$Myc$^{-/-}$) littermates to give rise to pups that are IGFBP-3KO but half of them will carry Myc transgene. IGFBP-3 WT:Myc (IGFBP-$3^{+/+}$Myc$^{+/-}$) of F2 will be mated with IGFBP-3WT (IGFBP-$3^{+/+}$Myc$^{-/-}$) littermates to give rise to pups that are IGFBP-3 WT but half of them will carry Myc transgene. The genotypes of all offspring were analyzed by PCR with genomic DNA isolated from ear and tail clippings using the following primer pairs: For Myc-5′ATGATAGCATCTTGTTCTTAGTCTTTTTCTTAATAGGG3′ and 5′GGTATCTGGACCTCACTGA CAAGGTGCAGAG3′ (PCR product will consist of two bands 400bp and 200bp). For IGFBP-3KO- 5′TAAGGTTCTCCAGACCTCAAAGTG3′ and 5′CCCTAGGAATGCTCGTCAAGA3′ (PCR product= 288bps). For IGFBP-3WT- 5′ TGCAGGCAGCCTAAGCACCTACCTC3′ and 5′ CCCAGGGTCCATTTTCCAACCTT3′ (PCR product= 164bps). Only the male IGFBP-3KO:Myc and IGFBP-3WT:Myc of F4 or later generations were used for experiments.

Biochemical Analysis

Mouse circulating IGF-1 and IGFBP-3 were measured using an in-house generated ELISA as previously described (18). Antibody and standard for IGF-1 and IGFBP-3 were obtained from R&D Systems (Minneapolis, MN).

Tissue RNA isolation and RT-PCR

Total RNA was isolated from 80-week-old male WT:Myc prostate and lung tissue and from IGFBP-3KO:Myc prostate and lung metastasis using Trizol reagent following the manufacturer's protocol (Invitrogen, Carlsbad, CA) followed by purification using the Qiagen RNeasy kit (Qiagen, Valencia, CA). One microgram of total RNA was treated with DNAse I and reverse transcribed using Superscript III and oligo dT following the manufacturer recommendations (Invitrogen, Carlsbad, CA). Human c-myc 420bp fragment and mouse GAPDH 600bp fragment were amplified by standard PCR using 5′ hotmastermix (5 prime, Gaithersburg, MD) and specific primers. Primers for human c-myc were 5′-CTCCTGGCAAAAGGTCAGAG-3′ (forward) and 5′-AGCTTTTGCTCCTCTGCTTG-3′ (reverse). Primers for mouse GAPDH were 5′-TTCACCACCATGGAGAAGGC-3′ (forward) and 5′-GAGGAAATGAGCTTGACAAA-3′ (reverse). The PCR conditions were as follows: 94°C for 3min; 94°C1min, 50°C 1min, 72°C 1min for 35 cycles followed by 10min at 72°C for final elongation using a Peltier thermal cycler PTC 200 (MJ Research, Waltham, MA). PCR products were run on a 1.5% agarose/ Ethidium Bromide gel.

Initiation and isolation of WT:Myc and IGFBP-3KO:Myc mouse primary prostate cancer cell lines

WT:Myc and IGFBP-3KO:Myc mouse primary prostate cancer cell lines were derived from two each of 37-week-old WT:Myc and IGFBP-3KO:Myc mice. The different lobes of prostate tumor were dissected under the dissecting microscope and then transferred to DMEM containing 10% fetal bovine serum plus 100 μg/ml penicillin and 100 μg/ml streptomycin. After washing with PBS 3 times, the tumor tissues were cut into 1 mm^3 pieces and incubated with collagenase for 1 hour to eliminate fibroblast contamination in the 37°C incubator containing 5% CO2. The cells were resuspended in DMEM containing 10% fetal bovine serum and 0.1 nM R1881 after centrifugation at 800×g for 5 min and grown as monolayers in flasks at 37°C with 90% humidity and 5% CO2. The culture medium was changed twice weekly until a confluent monolayer was established. The cells were passaged 4-10 times until use.

Immunoflourescence Confocal Microscopy

Thirty thousand cells per chamber were plated. Cells were fixed for 10 minutes in 4% paraformaldehyde in PBS and permeabilized in 0.2% Tween 20. Incubations with primary antibody and secondary reagent were done for 1 hour at room temperature. Endogenous IGFBP-3 was detected with anti-human IGFBP-3 goat polyclonal antibody (R&D Systems, Minneapolis, MN), followed by Alexa Fluor 488 (Molecular Probes, Carlsbad, CA). Counterstaining of nuclei was done with DAPI and cells were mounted in ProLong® Gold antifade reagent (Molecular Probes, Carlsbad, CA). Acquisitions were done using a Leica DM IRE2 Microscope and Leica Confocal Software.

Western Immunoblots

Protein extracts were prepared by homogenizing the cells in NP-40 lysis buffer supplemented with Complete Protease (Roche, Mannheim, Germany) and phosphatase inhibitors. Soluble proteins were boiled in 2×-SDS-sample buffer, resolved on a 4-20% Tris-HCl gel (Biorad, Hercules, CA), and transferred to PVDF membranes. Membranes were incubated with antibodies against Myc, E-cadherin, Vimentin (BD Biosciences, San Diego, CA); N-cadherin, Fibronectin, and SM22 (Abcam, Cambridge, MA); Smad4 (Cell Signaling, Danvers, MA); Androgen Receptor (AR) (Invitrogen, Carlsbad, CA); and β-actin (Sigma, St. Louis, MO). Membranes were incubated with horseradish peroxidase-linked secondary antibodies, washed and antigen-antibody complexes were visualized using enhanced chemiluminescence detection (Millipore, Billerica, MA).

In vitro invasion Assay

The ability of prostate cancer cells to invade was examined in 24-well cell culture chamber inserts (BD Matrigel Invasion Chamber, 8.0 Micron, BD Biosciences, Bedford, MA). WT:Myc and IGFBP-3KO:Myc mouse primary tumor cells were harvested by trypsinization, washed, and resuspended in phenol red–free medium containing 0.1% (w/v) bovine serum albumin. The number of living cells was counted using 0.4% trypan blue (Sigma, St. Louis, MO) exclusion. Only cells with viability ≥95% were used for further experiments. About 7×10^4 tumor cells in 200 μl of medium were added to the upper chamber with or without recombinant human IGFBP-3 (kind gift of INSMED Incorporated, Richmond, VA) in the concentrations indicated. The lower compartments were filled with 700 μl of conditioned medium, used as a chemoattractant, collected from 3×10^6 NIH/3T3 fibroblasts incubated overnight in growth medium containing 10% FCS. After 24 hours of incubation at 37°C under 5% CO2, the unattached cells in the upper chamber were swabbed and the invasive cells in the lower chamber were stained with 0.01% crystal violet, and then random fields were photographed under a microscope. After elution with 33% acetic acid,

absorbance was measured at 570 nm using an ELISA plate reader (Spectra MAX 190, Molecular Devices, Sunnyvale, CA).

Colony formation assay

WT:Myc and IGFBP-3KO:Myc lines were plated in triplicate in 60×15 mm grid plates (Fisher Scientifiç Pittsburgh, PA) at 1000 cells/well. Plates were subsequently incubated for 14 days in a humidified incubator at 37°C, and colonies were stained with 0.5 ml of 0.01% crystal violet solution for 10 min and counted using a dissecting microscope (50× magnification) for each triplicate sample. The average values are presented as mean ± SD.

In vitro cell growth kinetics

To determine cell growth kinetics, cells were grown in DMEM medium containing 10% fetal bovine serum and 0.1 nM R1881 (PerkinElmer Life Sciences, Boston, MA) in 96-well dishes at an initial density of 2,000 cells per well. Media was changed every three days. On days 1 through 5, cells were incubated with 10 μl of Cell Counting Kit-8 (CCK-8, Dojindo, Japan) for 3 hours, then absorbance at 450 nm was measured using an ELISA plate reader (Spectra MAX 190, Molecular Devices, Sunnyvale, CA).

Gene expression microarray analysis

Whole-genome expression analysis was performed with the Affymetrix Mouse Gene Array ST 1.0 (Affymetrix, Santa Clara, CA) at the UCLA DNA Microarray Core. RNA from WT:Myc and IGFBP-3KO:Myc primary prostate tumor cell lines was prepared using manufacturer recommended protocols and RNeasy (Qiagen, Valencia, CA) columns. Each sample was labeled using standard protocols and reagents from Affymetrix. Probes were fragmented and hybridized to the Affymetrix Human Gene 1.0 ST Array. Standard wash, stain, and scanning protocols were used.

Data analysis

GeneSpring GX 10.0.2 software (Agilent Technologies, Santa Clara, CA) was used to analyze the raw Excel files. The Exon RMA16 probe summarization algorithm, with a transcript level of core was used. The lower 20th percentile of the data was filtered out, leaving 23254/28815 transcripts. We compared the experimental group to the control group with a fold change of 3, to obtain lists of genes with differential expression. The genes were clustered with the following parameters: Clustering Algorithm: Hierarchical; Similarity Measure: Euclidean; Linkage Rule: Centroid. We used the DAVID program (19) to identify functional groups represented in these lists. Gene lists were tested for significant pathways using the MetaCore pathway web application by GeneGO, Inc. (St. Joseph, MI).

Statistics

All *in vitro* experiments were repeated at least three times. Means ± SD are shown. Statistical analyses were done using T-test, ANOVA, or Fisher's exact tests using InStat as indicated (GraphPad, San Diego, CA). Differences were considered statistically significant when $*P < 0.05$ and when $**P < 0.005$.

Results

IGFBP-3 is required for androgen deprivation-induced apoptosis

Multiple genes, including IGFBP-3 (20, 21) are upregulated in the prostate in response to androgen-deprivation; however, many of them (including Clusterin (22), and Bax (23)) have been shown not to be essential to prostatic apoptosis utilizing knockout mouse models. To assess the functional contribution of IGFBP-3 to prostate apoptosis in response to androgen-

deprivation we utilized the IGFBP-3 knockout (KO) mouse (17). Ten-week-old male wild type (WT) mice and IGFBP-3 KO mice were surgically castrated and prostates were harvested after 48 and 72 hours. The histological appearance of both testes and prostates from IGFBP-3 KO mice pre-castration did not differ from their control littermates at baseline as determined by H&E staining (data not shown). As expected, WT mouse prostates showed a dramatic 6-fold increase in the number of TUNEL-positive nuclei at 48 hours post castration (Figure 1A). However, IGFBP-3 KO mice prostates failed to show any significant increase in TUNEL staining at 48 hours. By 72 hours TUNEL staining returned to near baseline levels in WT mice and remained near baseline levels in IGFBP-3 KO mice. Serum IGFBP-3 levels were undetectable in the KO mouse and remained unchanged in WT mice post-castration (Figure 1B). Whereas data are conflicting on whether apoptosis secondary to androgen ablation is modified in p53 deficient mice (24, 25), we have now shown that IGFBP-3, which is activated downstream of p53 (26), is required for this process.

We did not observe spontaneous prostate tumor development with aging in IGFBP3KO mice. However, the incidence of splenic lymphomas in female IGFBP3KO mice was 23%; no splenic lymphomas were observed in WT mice (data not shown).

Paradoxical progression of CaP in IGFBP3KO:Myc mice

To investigate the significance of endogenous IGFBP-3 in the development of prostate cancer *in vivo* we crossed IGFBP3KO mice with the Myc model of prostate cancer (expressing human c-*Myc* driven by a prostate specific promoter (16)). These Myc mice reliably develop murine prostatic intraepithelial neoplasia (PIN), then adenocarcinomas. Myc mice develop relatively slow-growing, non-metastatic tumors. Surprisingly, at 17 weeks of age, the majority of prostates of IGFBP3KO:Myc mice did not develop cancer and only displayed PIN while control Myc mice had well differentiated prostate cancer (Figure 2A). We measured serum IGF-1 levels in these mice and found that it was decreased by more than 40% in the IGFBP-3KO:Myc mice when compared with controls (Figure 2B), thus providing a possible mechanism for the decreased cancer observed in the knockout animals. This finding correlates well with clinical studies showing serum IGF-1 levels to be an important determinant of early CaP (12, 27) in humans and mice (28, 29). By 24 weeks of age, well-differentiated cancer was observed in all mice irrespective of IGFBP-3 status (Supp. Figure 1A). By 80 weeks of age, prostate carcinoma was observed in all mice; however, tumors tended to be bigger in IGFBP3KO:Myc mice (Supp. Figure 1B) with some very large tumors in IGFBP3KO:Myc mice, 20% of which weighed more than 4g (Supp. Figure 1C).

Increased metastasis in IGFBP-3KO:Myc mice

When IGFBP-3KO:Myc mice were necropsied at 80 weeks of age, prostate tumors tended to be larger in the IGFBP-3KO:Myc mice when compared with WT (Supp. Figure 1B). In addition, we identified lung metastases in 55% of IGFBP-3KO:Myc mice, while none of the WT:Myc mice exhibited any metastases (Figure 3A, 3B). This is a remarkable finding, as metastases in the Myc model of prostate cancer have not been described to date, and suggests a major anti-tumorigenic role for endogenous IGFBP-3 as a metastasis suppressor. We characterized the presumptive lung metastases by immunohistochemical staining for Clara Cell 10 (CC10) protein, a marker of bronchiolar epithelial cells (30). CC10 is expressed in the lung in non-ciliated airway epithelial cells and is not expressed in prostate cells. Most primary lung adenomas and adenocarcinomas are of Clara cell origin.

As shown in Figure 4A, normal lung parenchyma stains positive for CC10, and the lung nodule does not, demonstrating that the observed lung nodules are not of lung origin.

Occasionally, some mice developed metastatic nodules in visceral organs including liver and intestine (Figure 3C, 3D). RT-PCR analysis for the human *Myc* gene verified expression in the lung nodules, thereby confirming their metastatic nature (Figure 4B).

Establishment and characterization of prostatic epithelial cell lines from the WT:Myc and IGFBP-3KO:Myc mouse models

To further our investigation of the molecular mechanisms underlying IGFBP-3-controlled prostate tumorigenesis and metastasis, we isolated primary prostatic cells from WT:Myc and IGFBP-3KO:Myc tumors. After serial passages (see Materials and Methods for details), several clonally derived cell lines were established and from which two lines each were characterized and studied herein. A representative cell line of each is presented. Confocal immunohistochemistry for IGFBP-3 confirmed absence of IGFBP-3 in the IGFBP3KO:Myc line (Supplemental Figure 2).

To determine the properties of these established cell lines, we performed Western blot analysis using antibodies corresponding to phenotypic markers in the prostate epithelium. As shown in Figure 5A, both WT:Myc and IGFBP-3KO:Myc cell lines maintained androgen receptor (AR) expression. Protein expression of E-cadherin (31) did not change and IGFBP-3KO:Myc phenotype was associated with a loss of Fibronectin expression. Expression of N-cadherin (32) increased with decrease in expression of Smad4 (33). This change in markers is consistent with the more aggressive phenotype of the IGFBP-3KO:Myc cells. In addition, Vimentin, a well-known marker of epithelial-mesenchymal transition (34), was significantly induced in the IGFBP-3KO:Myc cell line. Whereas many of the observed EMT markers are consistent with the more invasive phenotype of the IGFBP-3KO:Myc cells (Vimentin, N-Cadherin, Smad4), others are not consistent (E-Cadherin, Fibronectin); implying a complex contribution of IGFBP-3 loss to EMT that may be complicated in part by low serum IGF-1 levels (35).

To measure the biological effects of *IGFBP-3* gene deletion in *Myc* CaP cells, we first compared cell growth properties of the WT:Myc and IGFBP-3KO:Myc cell lines. As shown in Figure 5B, cell proliferation rates were significantly increased to over 3-fold at 120 hours in the IGFBP-3KO:Myc cell line as compared with WT:Myc cells, suggesting that IGFBP-3 plays a role in the cell cycle progression of *Myc* prostatic epithelial cells.

IGFBP-3 loss leads to increased colony formation and invasiveness of CaP cells *in vitro*

To determine whether genetic deletion of IGFBP-3 leads to enhanced transformation potential, we compared the colony forming efficiency of WT:Myc and IGFBP-3KO:Myc cell lines. After 14 days in culture, colonies were photographed and counted. IGFBP-3KO:Myc cells formed over 4-fold more colonies when compared with WT:Myc cells (Figure 6A).

In addition, to evaluate the relation between cell migratory ability and the expression of IGFBP-3, we conducted a migration assay using a modified Boyden chamber method. The invasiveness of IGFBP-3KO:Myc cells when compared with WT:Myc cells was increased over 3-fold (Figure 6B). In a separate experiment invasiveness was increased even more significantly in IGFBP-3KO:Myc cells when compared to WT:Myc cells. Addition of recombinant IGFBP-3 to IGFBP-3KO:Myc cells culture reversed this phenotype in a dose dependent manner (100 and 1000 ng/ml; Figure 6C). Thus taken together, these data support a role for IGFBP-3 in metastasis suppression in prostate cancer.

Differential Gene Expression in WT:Myc and IGFBP-3KO:Myc primary prostate tumor cell lines

Differential gene expression was examined using microarray analysis. Microarray analysis (28,815 genes) revealed that 462 genes were upregulated and 760 genes were downregulated (fold-change > 3.0; $P < 0.05$) (see Supplemental Table 1 for complete list; Figure 7A). Gene lists were tested for significant pathways using the MetaCore pathway web application by GeneGO, Inc. The most significant pathway maps were ranked by the negative log of the calculated hypergeometric p value. Genes differentially expressed fell into many different pathways but the two most significant pathways include cell adhesion and extracellular matrix remodeling, and development/regulation of epithelial-to-mesenchymal (EMT) transition, important pathways in the development of cancer metastasis (Figure 7B). SM22 (also known as Transgelin) was down-regulated 60-fold in IGFBP-3KO:Myc cells compared to WT:Myc cells in the array. A significant decrease in SM22 expression was confirmed by immunoblot (Figure 7C). SM22 is an actin cross-linking protein and functions as a tumor suppressor. Its expression in prostate cancer is decreased (36).

Discussion

The tumor-suppressive properties of IGFBP-3 have been intensely studied in our laboratory and by others *in vitro* and include IGF sequestration (6); mediation of anti-growth signals (37, 38); induction of cancer cell apoptosis (39); senescence-association (7); and its effects as an anti-angiogenic agent (11). Molecular mechanisms underlying these effects in CaP cells include rapid cellular internalization via Caveolin-1 binding and nuclear localization (40, 41); and activation of the intrinsic apoptosis pathway via association with the nuclear receptors RXRα and Nur77 and nuclear export with subsequent mitochondrial translocation (39, 42, 43). Importantly, we have established an important physiologic role for IGFBP-3 in apoptosis induced by androgen-deprivation.

Recent studies have hinted at a role for IGFBP-3 as a metastasis suppression gene. In a study of ovarian epithelial cancer (OEC) cell with invasion-related sublines, microarray analysis revealed IGFBP-3 to be one of the most suppressed genes in the most invasive subline P4. Re-expression of IGFBP-3 in P4 effectively inhibited cell migration, invasion and metastasis, but did not affect cell proliferation. In patients with EC tumors, low IGFBP-3 expression correlated clinically with higher tumor grade, advanced stage and poor survival (44). Moreover, in non-small cell lung cancer (NSCLC) cells, non-cytotoxic doses of adenoviral or recombinant IGFBP-3 significantly decreased the migration, invasion, and metastatic potential of H1299 and A549 NSCLC cells *in vitro* and *in vivo* (45). Furthermore, in patients with previously untreated metastatic colorectal cancer, higher baseline circulating levels of IGFBP-3 were associated with a significantly greater response rate to chemotherapy and a longer time to tumor progression and overall survival, even after adjusting for other potential predictors of patient outcome (46).

In men with prostate cancer, plasma IGFBP-3 levels were lowest in patients with bone metastases with lower preoperative IGFBP-3 levels and biopsy Gleason score being independent predictors of biochemical progression and failure related to cancer aggressiveness (14). Importantly, an A/C polymorphism at position -202 in the promoter region of IGFBP-3 was correlated to increased risk of metastatic disease in a Japanese study, with those men with CC and AC genotype having a significantly increased risk of metastatic disease (stage D) those with AA genotype. Therefore, the authors concluded that the presence of the C allele may cumulatively increase the risk for tumor metastasis and for having tumors with a biologically more aggressive phenotype (15).

In genetic mouse models of prostate cancer, many are aggressive and metastasize at an early age. These include: prostate PTEN deletion (12-29 weeks; (47)); TRAMP (12 weeks; (48)); and prostatic p53 and Rb inactivation (28 weeks; (49)). However, of the published genetic studies utilizing the Myc mouse, none have reported metastasis (16, 50, 51), making our observation of metastasis in IGFBP-3KO:Myc mice remarkable. Interestingly, a list of 18 prostate cancer 'signature' genes delineated in metastasis-prone prostatic p53 and Rb inactivated mice (49) includes the IGFBP-3 binding partner Caveolin-1 (40); the polycomb protein EZH2 that is known to repress IGFBP-3 expression (52, 53); the proto-oncogene and IGFBP-3 regulator Myb (54); and the homeobox tumor suppressor NKX3.1 that activates IGFBP-3 expression and whose actions are partially mediated by IGFBP-3 (55).

These important findings expand and confirm a novel role for IGFBP-3 (previously considered to function as a tumor suppressor), as an anti-metastasis gene, further supporting the targeting of IGFBP-3 as therapy in prostate cancer patients. Clearly, IGFBP-3 expression could represent a common signaling nexus in the CaP tumor suppression and further work into the molecular mechanisms that underlie its tumor suppressive effects may reveal targets for therapy in men with prostate cancer.

Supplementary Material

Refer to Web version on PubMed Central for supplementary material.

Acknowledgments

The authors acknowledge Ascia Eskin from the UCLA Microarray CORE for technical skill and helpful discussions.

Financial Support: Support for this project was received from P30DK063491 and R01AG20954 (PC), P50CA92131 (PC and KWL), K12HD34610 and DOD award PC061077 (KWL).

References

1. Hanahan D, Weinberg RA. The hallmarks of cancer. Cell. 2000; 100:57–70. [PubMed: 10647931]
2. Nelson WG, De Marzo AM, Isaacs WB. Prostate cancer. N Engl J Med. 2003; 349:366–81. [PubMed: 12878745]
3. Berthold DR, Pond GR, Soban F, de Wit R, Eisenberger M, Tannock IF. Docetaxel plus prednisone or mitoxantrone plus prednisone for advanced prostate cancer: updated survival in the TAX 327 study. J Clin Oncol. 2008; 26:242–5. [PubMed: 18182665]
4. Kantoff PW, Higano CS, Shore ND, Berger ER, Small EJ, Penson DF, et al. Sipuleucel-T immunotherapy for castration-resistant prostate cancer. The New England journal of medicine. 2010; 363:411–22. [PubMed: 20818862]
5. Yamada PM, Lee KW. Perspectives in mammalian IGFBP-3 biology: local vs. systemic action. Am J Physiol Cell Physiol. 2009; 296:C954–76. [PubMed: 19279229]
6. Nickerson T, Huynh H, Pollak M. Insulin-like growth factor binding protein-3 induces apoptosis in MCF7 breast cancer cells. Biochem Biophys Res Commun. 1997; 237:690–3. [PubMed: 9299428]
7. Schwarze SR, DePrimo SE, Grabert LM, Fu VX, Brooks JD, Jarrard DF. Novel pathways associated with bypassing cellular senescence in human prostate epithelial cells. J Biol Chem. 2002; 277:14877–83. [PubMed: 11836256]
8. Massoner P, Colleselli D, Matscheski A, Pircher H, Geley S, Durr P Jansen, et al. Novel mechanism of IGF-binding protein-3 action on prostate cancer cells: inhibition of proliferation, adhesion, and motility. Endocr Relat Cancer. 2009; 16:795–808. [PubMed: 19509068]
9. Thelen P, Burfeind P, Grzmil M, Voigt S, Ringert RH, Hemmerlein B. cDNA microarray analysis with amplified RNA after isolation of intact cellular RNA from neoplastic and non-neoplastic prostate tissue separated by laser microdissections. Int J Oncol. 2004; 24:1085–92. [PubMed: 15067329]

10. Liu B, Lee KW, Li H, Ma L, Lin GL, Chandraratna RA, et al. Combination therapy of insulin-like growth factor binding protein-3 and retinoid X receptor ligands synergize on prostate cancer cell apoptosis in vitro and in vivo. Clin Cancer Res. 2005; 11:4851–6. [PubMed: 16000583]
11. Liu B, Lee KW, Anzo M, Zhang B, Zi X, Tao Y, et al. Insulin-like growth factor-binding protein-3 inhibition of prostate cancer growth involves suppression of angiogenesis. Oncogene. 2007; 26:1811–9. [PubMed: 16983336]
12. Chan JM, Stampfer MJ, Giovannucci E, Gann PH, Ma J, Wilkinson P, et al. Plasma insulin-like growth factor-I and prostate cancer risk: a prospective study. Science. 1998; 279:563–6. [PubMed: 9438850]
13. Chan JM, Stampfer MJ, Ma J, Gann P, Gaziano JM, Pollak M, et al. Insulin-like growth factor-I (IGF-I) and IGF binding protein-3 as predictors of advanced-stage prostate cancer. J Natl Cancer Inst. 2002; 94:1099–106. [PubMed: 12122101]
14. Shariat SF, Lamb DJ, Kattan MW, Nguyen C, Kim J, Beck J, et al. Association of preoperative plasma levels of insulin-like growth factor I and insulin-like growth factor binding proteins-2 and -3 with prostate cancer invasion, progression, and metastasis. J Clin Oncol. 2002; 20:833–41. [PubMed: 11821468]
15. Wang L, Habuchi T, Tsuchiya N, Mitsumori K, Ohyama C, Sato K, et al. Insulin-like growth factor-binding protein-3 gene -202 A/C polymorphism is correlated with advanced disease status in prostate cancer. Cancer Res. 2003; 63:4407–11. [PubMed: 12907612]
16. Ellwood-Yen K, Graeber TG, Wongvipat J, Iruela-Arispe ML, Zhang J, Matusik R, et al. Myc-driven murine prostate cancer shares molecular features with human prostate tumors. Cancer Cell. 2003; 4:223–38. [PubMed: 14522256]
17. Yamada PM, Mehta HH, Hwang D, Roos KP, Hevener AL, Lee KW. Evidence of a Role for Insulin-Like Growth Factor Binding Protein (IGFBP)-3 in Metabolic Regulation. Endocrinology.
18. Hwang DL, Lee PD, Cohen P. Quantitative ontogeny of murine insulin-like growth factor (IGF)-I, IGF-binding protein-3 and the IGF-related acid-labile subunit. Growth Horm IGF Res. 2008; 18:65–74. [PubMed: 17719253]
19. Huang da W, Sherman BT, Lempicki RA. Systematic and integrative analysis of large gene lists using DAVID bioinformatics resources. Nat Protoc. 2009; 4:44–57. [PubMed: 19131956]
20. Nickerson T, Miyake H, Gleave ME, Pollak M. Castration-induced apoptosis of androgen-dependent shionogi carcinoma is associated with increased expression of genes encoding insulin-like growth factor-binding proteins. Cancer Res. 1999; 59:3392–5. [PubMed: 10416600]
21. Bruyninx M, Ammar H, Reiter E, Cornet A, Closset J. Genes upregulated during castration-induced rat prostatic apoptosis: cloning and characterization of new cDNAs. BJU Int. 2000; 85:1134–42. [PubMed: 10848710]
22. Fink D, Fazli L, Aronow B, Gleave ME, Ong CJ. Clusterin is not essential for androgen-regulated involution and regeneration of the normal mouse prostate. Prostate. 2006; 66:1445–54. [PubMed: 16865725]
23. Bruckheimer EM, Cho S, Brisbay S, Johnson DJ, Gingrich JR, Greenberg N, et al. The impact of bcl-2 expression and bax deficiency on prostate homeostasis in vivo. Oncogene. 2000; 19:2404–12. [PubMed: 10828882]
24. Berges RR, Furuya Y, Remington L, English HF, Jacks T, Isaacs JT. Cell proliferation, DNA repair, and p53 function are not required for programmed death of prostatic glandular cells induced by androgen ablation. Proc Natl Acad Sci U S A. 1993; 90:8910–4. [PubMed: 8415631]
25. Colombel M, Radvanyi F, Blanche M, Abbou C, Buttyan R, Donehower LA, et al. Androgen suppressed apoptosis is modified in p53 deficient mice. Oncogene. 1995; 10:1269–74. [PubMed: 7731676]
26. Buckbinder L, Talbott R, Velasco-Miguel S, Takenaka I, Faha B, Seizinger BR, et al. Induction of the growth inhibitor IGF-binding protein 3 by p53. Nature. 1995; 377:646–9. [PubMed: 7566179]
27. Nimptsch K, Platz EA, Pollak MN, Kenfield SA, Stampfer MJ, Willett WC, et al. Plasma insulin-like growth factor 1 is positively associated with low-grade prostate cancer in the Health Professionals Follow-up Study 1993-2004. Int J Cancer.

28. Silha JV, Sheppard PC, Mishra S, Gui Y, Schwartz J, Dodd JG, et al. Insulin-like growth factor (IGF) binding protein-3 attenuates prostate tumor growth by IGF-dependent and IGF-independent mechanisms. Endocrinology. 2006; 147:2112–21. [PubMed: 16469805]
29. Cohen P. Insulin-like growth factor binding protein-3: insulin-like growth factor independence comes of age. Endocrinology. 2006; 147:2109–11. [PubMed: 16617154]
30. Lee KS, Lee YS, Lee JM, Ito K, Cinghu S, Kim JH, et al. Runx3 is required for the differentiation of lung epithelial cells and suppression of lung cancer. Oncogene. 29:3349–61. [PubMed: 20228843]
31. Jeanes A, Gottardi CJ, Yap AS. Cadherins and cancer: how does cadherin dysfunction promote tumor progression? Oncogene. 2008; 27:6920–9. [PubMed: 19029934]
32. Tanaka H, Kono E, Tran CP, Miyazaki H, Yamashiro J, Shimomura T, et al. Monoclonal antibody targeting of N-cadherin inhibits prostate cancer growth, metastasis and castration resistance. Nat Med. 2010; 16:1414–20. [PubMed: 21057494]
33. Ding Z, Wu CJ, Chu GC, Xiao Y, Ho D, Zhang J, et al. SMAD4-dependent barrier constrains prostate cancer growth and metastatic progression. Nature. 2011; 470:269–73. [PubMed: 21289624]
34. Lee JM, Dedhar S, Kalluri R, Thompson EW. The epithelial-mesenchymal transition: new insights in signaling, development, and disease. J Cell Biol. 2006; 172:973–81. [PubMed: 16567498]
35. Graham TR, Zhau HE, Odero-Marah VA, Osunkoya AO, Kimbro KS, Tighiouart M, et al. Insulin-like growth factor-I-dependent up-regulation of ZEB1 drives epithelial-to-mesenchymal transition in human prostate cancer cells. Cancer research. 2008; 68:2479–88. [PubMed: 18381457]
36. Prasad PD, Stanton JA, Assinder SJ. Expression of the actin-associated protein transgelin (SM22) is decreased in prostate cancer. Cell Tissue Res. 2010; 339:337–47. [PubMed: 20012321]
37. Rajah R, Valentinis B, Cohen P. Insulin-like growth factor (IGF)-binding protein-3 induces apoptosis and mediates the effects of transforming growth factor-beta1 on programmed cell death through a p53- and IGF-independent mechanism. J Biol Chem. 1997; 272:12181–8. [PubMed: 9115291]
38. Harms KL, Chen X. The C terminus of p53 family proteins is a cell fate determinant. Mol Cell Biol. 2005; 25:2014–30. [PubMed: 15713654]
39. Lee KW, Ma L, Yan X, Liu B, Zhang XK, Cohen P. Rapid apoptosis induction by IGFBP-3 involves an insulin-like growth factor-independent nucleomitochondrial translocation of RXRalpha/Nur77. J Biol Chem. 2005; 280:16942–8. [PubMed: 15731112]
40. Lee KW, Liu B, Ma L, Li H, Bang P, Koeffler HP, et al. Cellular internalization of insulin-like growth factor binding protein-3: distinct endocytic pathways facilitate re-uptake and nuclear localization. J Biol Chem. 2004; 279:469–76. [PubMed: 14576164]
41. Burrows C, Holly JM, Laurence NJ, Vernon EG, Carter JV, Clark MA, et al. Insulin-like growth factor binding protein 3 has opposing actions on malignant and nonmalignant breast epithelial cells that are each reversible and dependent upon cholesterol-stabilized integrin receptor complexes. Endocrinology. 2006; 147:3484–500. [PubMed: 16614079]
42. Lee KW, Cobb LJ, Paharkova-Vatchkova V, Liu B, Milbrandt J, Cohen P. Contribution of the orphan nuclear receptor Nur77 to the apoptotic action of IGFBP-3. Carcinogenesis. 2007; 28:1653–8. [PubMed: 17434920]
43. Paharkova-Vatchkova V, Lee KW. Nuclear export and mitochondrial and endoplasmic reticulum localization of IGF-binding protein 3 regulate its apoptotic properties. Endocr Relat Cancer. 17:293–302. [PubMed: 20228135]
44. Torng PL, Lee YC, Huang CY, Ye JH, Lin YS, Chu YW, et al. Insulin-like growth factor binding protein-3 (IGFBP-3) acts as an invasion-metastasis suppressor in ovarian endometrioid carcinoma. Oncogene. 2008; 27:2137–47. [PubMed: 17952116]
45. Oh SH, Lee OH, Schroeder CP, Oh YW, Ke S, Cha HJ, et al. Antimetastatic activity of insulin-like growth factor binding protein-3 in lung cancer is mediated by insulin-like growth factor-independent urokinase-type plasminogen activator inhibition. Mol Cancer Ther. 2006; 5:2685–95. [PubMed: 17121915]
46. Fuchs CS, Goldberg RM, Sargent DJ, Meyerhardt JA, Wolpin BM, Green EM, et al. Plasma insulin-like growth factors, insulin-like binding protein-3, and outcome in metastatic colorectal

cancer: results from intergroup trial N9741. Clin Cancer Res. 2008; 14:8263–9. [PubMed: 19073970]

47. Wang S, Gao J, Lei Q, Rozengurt N, Pritchard C, Jiao J, et al. Prostate-specific deletion of the murine Pten tumor suppressor gene leads to metastatic prostate cancer. Cancer Cell. 2003; 4:209–21. [PubMed: 14522255]
48. Gingrich JR, Barrios RJ, Morton RA, Boyce BF, DeMayo FJ, Finegold MJ, et al. Metastatic prostate cancer in a transgenic mouse. Cancer Res. 1996; 56:4096–102. [PubMed: 8797572]
49. Zhou Z, Flesken-Nikitin A, Corney DC, Wang W, Goodrich DW, Roy-Burman P, et al. Synergy of p53 and Rb deficiency in a conditional mouse model for metastatic prostate cancer. Cancer Res. 2006; 66:7889–98. [PubMed: 16912162]
50. Iwata T, Schultz D, Hicks J, Hubbard GK, Mutton LN, Lotan TL, et al. MYC overexpression induces prostatic intraepithelial neoplasia and loss of Nkx3.1 in mouse luminal epithelial cells. PLoS One. 5:e9427. [PubMed: 20195545]
51. Nandana S, Ellwood-Yen K, Sawyers C, Wills M, Weidow B, Case T, et al. Hepsin cooperates with MYC in the progression of adenocarcinoma in a prostate cancer mouse model. Prostate. 70:591–600. [PubMed: 19938013]
52. Tan J, Yang X, Zhuang L, Jiang X, Chen W, Lee PL, et al. Pharmacologic disruption of Polycomb-repressive complex 2-mediated gene repression selectively induces apoptosis in cancer cells. Genes Dev. 2007; 21:1050–63. [PubMed: 17437993]
53. Dimri M, Bommi PV, Sahasrabuddhe AA, Khandekar JD, Dimri GP. Dietary omega-3 polyunsaturated fatty acids suppress expression of EZH2 in breast cancer cells. Carcinogenesis. 31:489–95. [PubMed: 19969553]
54. Kim MS, Kim SY, Arunachalam S, Hwang PH, Yi HK, Nam SY, et al. c-myb stimulates cell growth by regulation of insulin-like growth factor (IGF) and IGF-binding protein-3 in K562 leukemia cells. Biochem Biophys Res Commun. 2009; 385:38–43. [PubMed: 19427836]
55. Muhlbradt E, Asatiani E, Ortner E, Wang A, Gelmann EP. NKX3.1 activates expression of insulin-like growth factor binding protein-3 to mediate insulin-like growth factor-I signaling and cell proliferation. Cancer Res. 2009; 69:2615–22. [PubMed: 19258508]

Precis: This study reports the first transgenic mouse model of spontaneous metastatic prostate cancer, a milestone that may help advance studies of progression and treatment at this deadly late stage of disease.

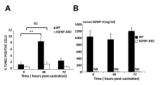

Figure 1.
(A) TUNEL quantitation was by counting 500 cells per field in five random fields per section (n=6/genotype). Control littermate (dark) and IGFBP-3KO (light). **p<0.005 by T-test. (B) Serum IGFBP-3 levels were unchanged post-castration in WT mice and remain undetectable in IGFBP-3KO mice. ND = Not detected.

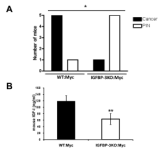

Figure 2.

(A) Paradoxical progression of CaP in IGFBP-3KO:Myc mice. Incidence of Prostatic Intraepithelial Neoplasia (PIN) and adenocarcinoma in 17-week-old male WT:Myc and IGFBP-3KO:Myc mice. *p<0.05 by Fisher's Exact Test. (B) Serum IGF-1 levels in 17-week-old male WT:Myc and IGFBP-3KO:Myc mice. **p<0.005 by T-Test.

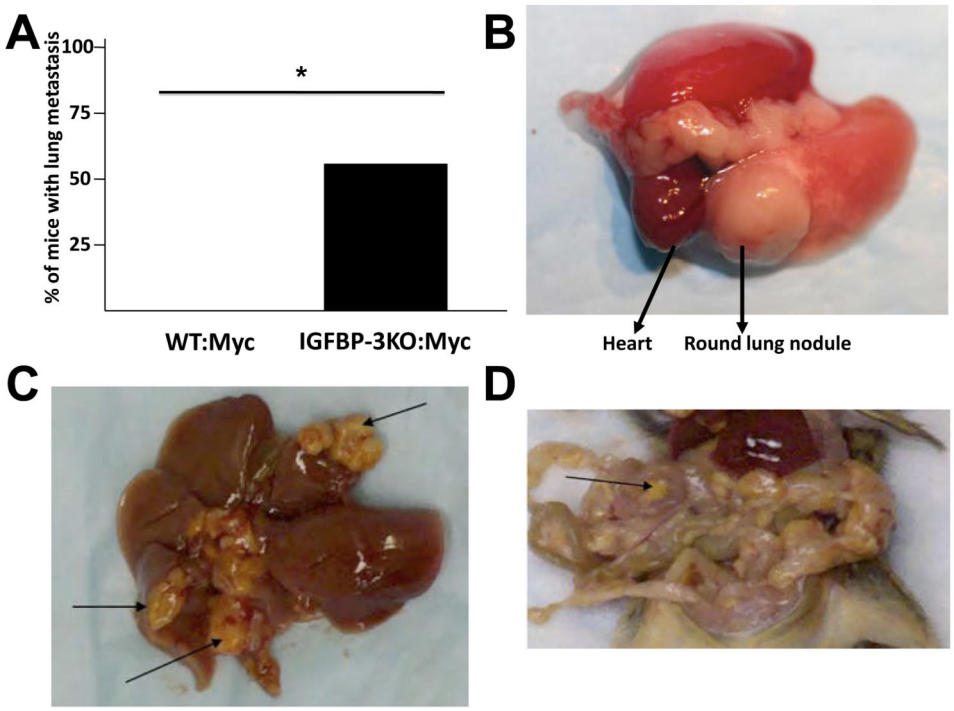

Figure 3.

(A) Increased metastasis in IGFBP-3KO:Myc mice. Incidence of lung metastases in 80-week-old WT:Myc (n=22) and IGFBP-3KO:Myc (n=18) male mice. *p<0.05 by Fisher's Exact Test. (B) Representative photograph of lung nodule. (C) Multiple metastases in liver (arrows). (D) Multiple metastases in intestine (arrow pointing at one of many).

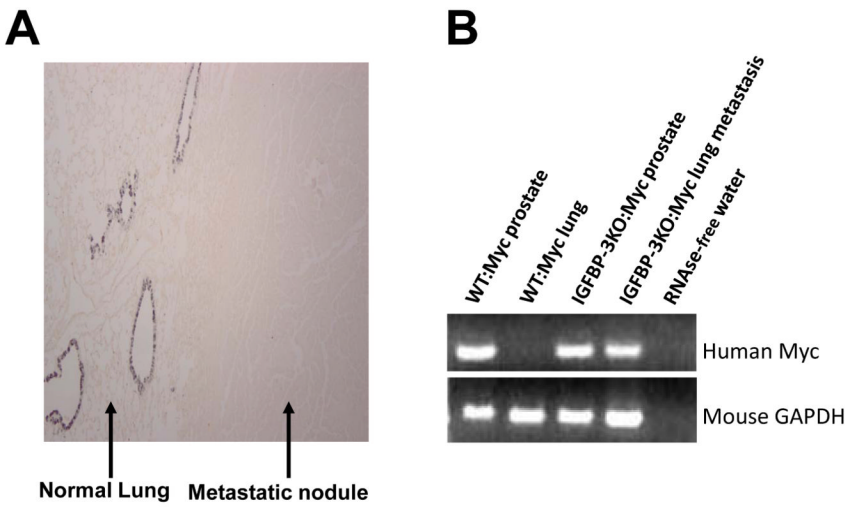

Figure 4.

(A) CC10 immunohistochemical staining of a representative lung nodule and adjacent normal lung tissue in a IGFBP-3KO:Myc mouse. (B) RT-PCR of human Myc of primary tissue RNA from mouse necropsy confirming metastatic nature of lung nodules.

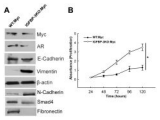

Figure 5.

(A) Expression of characteristic proteins in primary WT:Myc and IGFBP-3KO:Myc cell lines by Western immunoblot. (B) Cell proliferation curves of WT:Myc and IGFBP-3KO:Myc cell lines by MTT assay. *$p<0.05$ for entire curves by ANOVA.

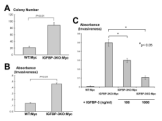

Figure 6.

(A) Increased colony formation in IGFBP-3KO:Myc cells $p<0.01$ by T-Test. (B) Increased invasiveness of IGFBP-3KO:Myc cells. $p<0.01$ by T-Test. (C) Addition of recombinant human IGFBP-3 to IGFBP-3KO:Myc cell line reverses invasive phenotype. **$p<0.05$ by T-test.

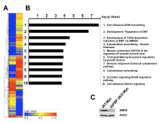

Figure 7.

(A) Heat map of representative IGFBP-3KO:Myc tumor gene expression (left column) and WT:Myc tumor gene expression (right column). The 6.9 and 11.5 range = $\log_2$ transformed value of the RNA normalized intensity values. For the part of the heatmap where the experiment is yellow and the controls are blue, those genes are down-regulated in the controls. This is also the case for when the experiment is red and the controls are yellow and blue. For the genes where the control is blue and the experiment are yellow to red, these genes are up-regulated in the controls. (B) Significant pathway maps ranked by the negative log of the calculated hypergeometric p value (C) Downregulation of SM22 expression in IGFBP-3KO:Myc cells as compared to WT:Myc cells as measured by Western immunoblot.